Real-Time Tactile Grasp Force Sensing Using Fingernail Imaging via Deep Neural Networks

Navid Fallahinia[1] and Stephen A. Mascaro[1]

***Abstract*— This paper has introduced a novel approach for the real-time estimation of 3D tactile forces exerted by human fingertips via vision only. The introduced approach is entirely monocular vision-based and does not require any physical force sensor. Therefore, it is scalable, non-intrusive, and easily fused with other perception systems such as body pose estimation, making it ideal for HRI applications where force sensing is necessary. The introduced approach consists of three main modules: finger tracking for detection and tracking of each individual finger, image alignment for preserving the spatial information in the images, and the force model for estimating the 3D forces from coloration patterns in the images. The model has been implemented experimentally, and the results have shown a maximum RMS error of 8.4% (for the entire range of force levels) along all three directions. The estimation accuracy is comparable to the offline models in the literature, such as EigneNail, while, this model is capable of performing force estimation at 30 frames per second.**

I. INTRODUCTION

Human-Robot Interaction (HRI) has recently received considerable attention in the robotics community and have enabled new applications which previously only humans could perform, such as object manipulation [1], [2], assistive devices and rehabilitation technology [3], [4], and inferring human intent for collaborative robots [5], [6]. More recently, with advances in computer vision, many studies have started focusing on vision-based HRI (vHRI) to recognize and anticipate human actions during interactions with robots [7], [8]. Among those, anticipation is a critical aspect of an HRI system, enabling it to update its observed belief about their surrounding actions and predict them before happening, which reduces the intelligent system's cognitive load for executing any reactive responses.

There have been several works on human actions anticipation in HRI by monitoring body and hand poses. The main focus of these approaches is action anticipation via kinematic pose estimation using either a single image [9], [10] or video sequences [11], [12]. In some cases, body/hand motion trajectories are also used for anticipation [13]. Even though there is considerable research on vision-based action analysis during object manipulation, there are still many grasp configurations that are not predictable using vision-based methods alone. For instance, if a person is passing an object to a robot manipulator, it needs to know the hand-object interaction forces in order to prepare for the appropriate action to receive it. This requires sensing the hand's tactile force vectors, which, however, cannot be directly inferred from the hand pose. It has been shown that a near-identical hand kinematic pose can correspond to multiple different grasp taxonomies such as power grasp vs. precision grasp. Therefore, the only distinct feature is tactile force vectors, making them an essential feature to consider when parsing hand-object interactions from an HRI perspective.

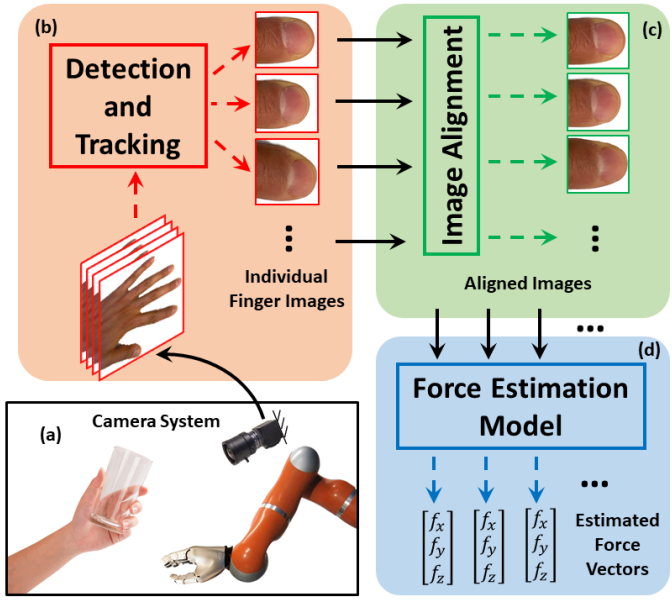

Fig. 1: Processing stages of the vision-based 3D force estimation model. (a) Image frames are captured by either a fixed or a moving (attached to a robotic arm) monocular camera. (b) Individual fingers are detected and tracked in each frame captured during the grasping task. (c) Each cropped fingertip image from the previous stage is aligned to desired geometrical shape. (d) The force model maps the aligned images to a 3D force vector by investigating the coloration features

In applications where the physical interaction is mediated through a third object, force measurement is traditionally done either via instrumented objects [14], or through wearable devices [15]. However, these existing solutions are often not feasible to be applied to real-world applications as they are costly, not scalable, intrusive, and may impose a set of restrictions on where the humans can place their fingers [16]. Therefore, there is still no effective tactile grasp force-sensing method without requiring physical force sensors for

This work was partially supported by National Science Foundation (NSF) Grant NRI-1208626

Human subject research in this study has been approved by the University of Utah Institutional Review Board (IRB 00014064).

[1]Authors are with the Robotics Center, University of Utah, Salt Lake City, Utah, USA, n.fallahinia@utah.edu

HRI applications, where the robot might need to be aware of the human tactile forces exerted on a jointly manipulated object. To address this problem, we have developed a novel solution for non-intrusive real-time 3D tactile force estimation via imaging and by investigating the coloration pattern change in human fingernails when they grasp an object. Moreover, to overcome the problem of fingernail image variances, we trained an image alignment model that can compensate for rotation, translation, scaling in real-time. Additionally, on account of the fact that finger locations can be changing during a manipulation task, we implemented a finger detection and tracking model to ensure that all fingers can be visible all the time. In summary, the main contributions of our paper are to 1) propose an end-to-end DNN model for real-time 3D tactile force estimation from video frames 2) develop an image alignment model to avoid data loss and to increase the accuracy of the force estimation model 3) introduce a vision-based force-sensing framework that can be integrated with other perception modules for real-time monitoring of human-robot interactions 4) collect a large-scale dataset for human tactile force estimation from fingernail images, which includes thousands of fingernail images with 3D measured forces from multiple human subjects with different finger size, texture, and color.

II. Related work

Generally, force-sensing via fingernail imaging aims to estimate the 3D precision grasp forces that are typically employed during dexterous manipulation and involve only the finger pads [17]. The basic concept relies on the fingernail's coloration during contact with objects, where due to the blood flow changes in the fingertip and transparency of the fingernail, some distinguishable coloration patterns are created. Early approaches [18], [19] used stereo imaging to generate 3-D models of a fingernail. Then, 2-D images were registered to the model using markers or pattern grids on the fingernail. While this method was seen to be accurate, it was only able to estimate normal forces. Other approaches suggested using traditional rigid body transformation techniques such as the Harris feature points [20], Canny edge detection [21], and template matching [22] for registration and mapping to the force space. The main common drawback of all these approaches is that the entire image registration has to be done offline as a separate pre-processing step before force estimation, making it almost impossible for any real-time application in robotics.

Active Appearance Models (AAM) [23] has been proposed for 2D image registration along with EigenNail (based on eigenvalue analysis of the fingernail images) [24] for 3D force estimation. However, this approach requires each finger of each human subject to be calibrated individually [25]. This is a significant drawback since for every new human subject, a new training dataset must be collected, and the model must be retrained. In another recent work [26], Convolutional Neural Networks (CNN) were proposed for 2D-to-3D image registration followed by Gaussian processes for force and torque estimation on the fingertips. However, the experimental method in that work was limited, as it did not independently vary the 3D contact forces, leading to low accuracy for force estimation along all directions simultaneously. Moreover, this method requires a calibration marker attached to the fingers for estimating the force direction. More recently, Recurrent Neural Networks (RNN) have been suggested for learning a mapping between the high-level kinematic features of hand and the underlying manipulation forces using RGB-D images [27]. However, as it was mentioned before, different grasp force distributions can have identical kinematic hand poses, making predictions by this method inaccurate for many precision grasp cases.

III. Method Descriptions

In this work we address the problem of real-time 3D tactile force estimation via imaging in two levels: *force estimation* in the from of estimating forces from a single cropped fingernail image, and *detection and tracking* as a model for tracking each finger in multiple video frames (Fig. 1). The former is where the image of each detected fingernail is passed to an image alignment module followed by a DNN model to estimate the 3D forces. While, the later ensures that the right region of the finger is detected and being tracked during a grasping task, as there are multiple fingers in each frame.

A. Image Alignment

Image alignment is necessary to avoid any data loss due to the fingernail's possible translation and rotation on the captured frames. Generally speaking, the design of CNN can handle some slight transformations (pooling layers endow the DNN with some extent of spatial invariance as they act as a down-sampling mechanism). However, CNNs are not invariant to relatively large input distortions. Moreover, we use depth-wise separable convolution architecture to increase the real-time efficiency in this work, which does not use pooling layers. Therefore, we employed the idea of Spatial Transformer Network (STN) [28] for image alignment before encoding any coloration features from the fingernails.

STN was originally designed to increase image classification accuracy by compensating for the spatial transformations in the images using a learnable affine transformation. In the original implementation [28], Spatial Transformer (ST) module was applied at the intermediate feature map, and the affine transformation θ was learned simultaneously with the classification task. However, in this work, we use STN in a different framework, where first, a transformation module is learned by applying STN at the high-level feature map (we are only interested in the fingernail image not the background information). The learned ST module will be then applied to the input images at the force estimation step to warp them into the desired pose (as shown in Fig. 2).

To train the affine transformation in the STN, we first apply a CNN to the raw image to extract the high-level feature map. Then, the ST module will transform the feature map into a different warping. Finally, the distance between the transformed map and the feature map of the aligned images

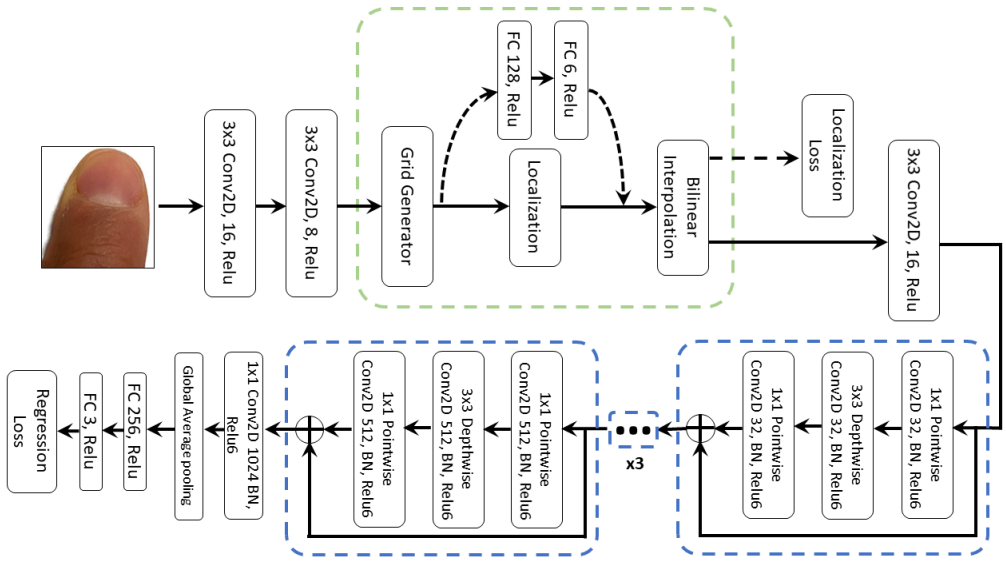

Fig. 2: The proposed fingertip 3D force estimation framework. The image alignment model receives as input a cropped fingernail image that was detected by the SSD. The high-level feature map of the image is initially extracted, then the learned transformation is applied by the ST module. A bi-linear interpolation will finally reconstruct the warped image. The coloration feature map is extracted from the aligned image through 5 blocks of depthwise separable convolutions. In the diagram, FC refers to fully-connected layers, BN refers to batch normalization, and $\oplus$ refers to concatenation. The ST layer is trained separately and then added to the force estimation model.

(constructed using AAM in [23]) is calculated through a $\mathcal{L}_2$ loss function as follows:

$$\mathcal{L}_{alig} = \sum_{n=1}^{N} \left\| I_{raw}^{(i)} - I_{aligned}^{(i)} \right\| \tag{1}$$

Where N is the batch size, I_{raw} is the raw image, and $I_{aligned}$ is the ground truth image aligned by AMM.

B. Force Estimation Model

The objective of the force estimation model is to estimate the three tactile force components f_x, f_y, and f_z exerted by the fingertip, given an aligned image $I_{aligned}^{(i)}$. Where f_z always corresponds to normal force, f_x corresponds to lateral force, and f_y corresponds to longitudinal force on the finger. As depicted in Fig. 2), The force estimation model has two parts. First, a CNN network extracts the coloration features on the images, including the patterns on both the nail and the surrounding skin. Then, a fully connected network will learn a nonlinear mapping between the feature space the 3D forces based on the following loss function:

$$\mathcal{L}_{force} = \sum_{n=1}^{N} \left\| F - \hat{F} \right\| \tag{2}$$

Where $\hat{F}$ and F are the estimated and measured force vectors, respectively.

The magnitude of the forces is estimated based on the pixel intensity of the coloration patterns. At the same time, the forces' direction is found based on the locations where those patterns appear. As an example, normal forces result in a whitening band near the distal end of the finger. It has also been shown that these patterns are common among different humans [29]. Therefore, it is essential to preserve the local spatial information during the feature extraction. Additionally, the model has to be computationally inexpensive to be used in real-time robotic applications. To address these problems, we use a similar architecture introduced in [30], which is based on using depthwise separable convolution blocks to perform the convolution operation very efficiently. Moreover, instead of using pooling layers, some depthwise blocks have a stride of 2 to reduce the spatial dimensions without losing much spatial information.

C. Finger Tracking

The alignment and estimation models are designed to receive a single fingernail image (the coloration region of interest is from the DIP joint to the very distal edge of the fingernail). However, during manipulation or grasping tasks, the camera looks at the entire human hand, meaning that there could be multiple fingers with different orientations in each frame. Thus, a detection and tracking system needs to be implemented to ensure that the force estimation module is receiving the appropriate image. To resolve this problem, we have implemented a fingernail detection and tracking model, which is based on Single Shot multi-box Detection (SSD) [31] algorithm and is trained on our annotated finger dataset. However, running a detection model at each frame will not be efficient; thus, we have applied a Multiple Instance Learning (MIL) tracker in addition to the finger detector. This way, the detection model needs to be called at every ten frames

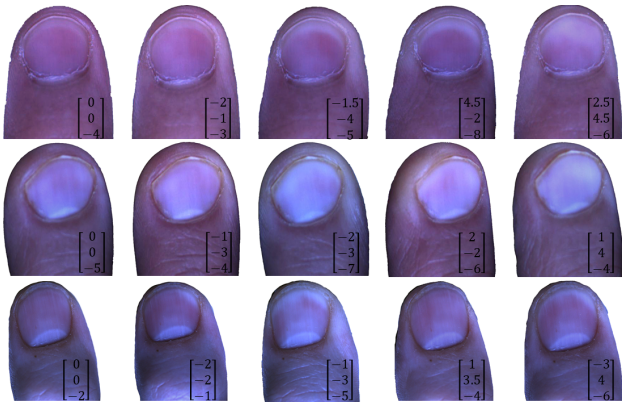

Fig. 3: A few examples of the fingernail images and 3D ground truth measured from multiple human subjects in the dataset.

Fig. 4: Qualitative results of the alignment model performance. (a) Raw images with different rotational and transnational variations. (b) warped images after image alignment.

or when the tracker loses the fingers.

IV. Experimental evaluation

A. Implementation

All three models, including the image alignment, force estimation, and finger detection, are trained separately and then combined at the inference time as one end-to-end model. We use Tensorflow 2 for the implementation of the training pipelines on an Nvidia TITAN RTX GPU. However, To improve the run-time performance, we use tensor-oriented linear quantization by mapping the floating-point real values to an 8-bit quantization space via ONNX [32]. The models were then exported to Nvidia TensorRT for GPU accelerated execution.

Image Alignment. In this step, we first train the localization network part of the ST module. Two Conv layers with 16 and 8 filters, kernel size of 3×3 with stride 1, and Relu activation function extract the high-level feature map. The localization network is a fully connected layer (FC) with 128 and 6 units, respectively. The grid generator and the bilinear interpolation units are implemented in the same way that described in [28]. Input images are resized to match the STN input size of 240×240. This model is trained using Adam optimizer with learning rate of 10^{-3} for 2500 epochs using a batch size of 32 with L2 regularization of 0.001.

Force Estimation. Once the alignment model has been trained, the weights will be frozen and incorporated with the force estimation model. The model includes a Conv layer with 16 filters, kernel size of 3×3 with stride 1 at the very first layer after the ST module. Then, an architecture similar to MobilenetV2 [30] (without the first and last layer), with different number of separable blocks, is applied on the aligned feature map. The regression module includes a Global Average Pooling followed by FC layers with 256 and 3 units, respectively. We also used dropout of 0.5 to prevent over-fitting. Raw images are resized to 242×242 to be compatible with the network dimensions. All the activation function are Relu6 with batch normalization. The force estimation model is trained using RMSProp optimizer with learning rate of 10^{-4} for 5000 epochs using a batch size of 32. For both models we report RMSE as the metric.

B. Dataset

The dataset includes 54000 raw fingernail images, aligned images, and measured forces that were collected from 18 human subjects including 6 females and 12 males with different finger and fingernail shapes, sizes, textures, and skin colors. For each human subject, the images of four fingers, including Thumb, Index, Middle, and Ring, were collected separately. Fig. 3 shows some examples from the dataset. The image collection and the force measurement procedures are explained in previous works [33] in detail. As it was noted before, the ground truth aligned images are generated using AAM as described in [29]. The dataset was divided into train, test, and validation sets with the ratios of 80%, 10%, and 10%, respectively. The SSD model for was trained on the 11k Hands dataset [34] that was annotated by our group for the finger detection task.

C. Results and Discussion

Fig. 4 shows some qualitative test results from the image alignment model. It can be seen that the model is cable of handling both rotational and translation transformations in the fingernail images. The base alignment model was trained only with the actual collected images (no augmentation added), which resulted in the average alignment error of 2.25 ± 0.3 (RMS pixel intensity error). It should be noted that we use a finger restraint at PIP joint during the data collection, which would limit the finger movement. While during grasping or manipulation, the finger can move more freely. Therefore, the geometric variations in the collected fingernail dataset are limited compared to a real-world grasping scenario; notably, there will be more rotation along the z axis and more translation along the x and y axes. To overcome this problem, we augmented the images in such a way that there would be random rotations by up to 30 degrees and random translations by up to 40% of the image size. The base alignment model was retrained with the augmented data, which resulted in the average alignment error of 3.63 ± 0.3 (RMS pixel intensity error) less than 1% of the range of 0-255. Although there is a slight change in the alignment error

TABLE I: Force estimation results achieved by different models. All the results are as mean RMS error ± two standard deviation ($\mu \pm \sigma$). All the errors are shown in (N). The columns represent the force estimation accuracy along each direction per finger, while each row shows the results for each model.

	Index			Middle			Ring			Thumb		
	F_z	F_x	F_y	F_z	F_x	F_y	F_z	F_x	F_y	F_z	F_x	F_y
EigenNail	0.57±0.02	0.43±0.01	0.41±0.01	0.52±0.04	0.41±0.03	0.40±0.02	0.54±0.03	0.43±0.02	0.42±0.01	0.53±0.03	0.44±0.03	0.43±0.02
Raw Images	1.94±0.08	1.52±0.07	1.55±0.07	1.54±0.06	1.32±0.04	1.19±0.04	1.51±0.06	1.30±0.03	1.27±0.04	1.57±0.07	1.36±0.05	1.41*pm*0.04
Aligned Images	0.77±0.03	0.62±0.02	0.64±0.02	0.74±0.03	0.59±0.03	0.60±0.02	0.75±0.02	0.61±0.01	0.58±0.02	1.53±0.06	1.17±0.05	1.24±0.05
Fingers Model	**0.58±0.03**	**0.43±0.02**	**0.42±0.02**	**0.56±0.03**	**0.43±0.03**	**0.45±0.02**	**0.53±0.03**	**0.44±0.03**	**0.42±0.02**	1.69±0.06	1.52±0.06	1.49±0.05
Thumb Model	1.81±0.07	1.52±0.05	1.55±0.06	1.57±0.06	1.17±0.05	1.25±0.05	1.49±0.06	1.19±0.04	1.21±0.05	**0.55±0.03**	**0.45±0.03**	**0.44±0.02**

after augmentation, the retrained model can handle more geometric transformations.

To study the performance of the force estimation model, we conducted multiple evaluations, which have been summarized in Table I. We first train the model with raw data without any image alignment. As it can be seen from Table I, the prediction errors have significantly increased (by an average of 30%) compared to the results from the EigneNail model [16]. It clearly indicates that image alignment is essential to prevent data loss and ensure that the force estimation model compares the same locations of the finger from one image to the next. Therefore, we added the alignment module to the estimation model, which converts both train and test images into an aligned configuration before force prediction. According to Table I, the force estimation error reduces by an average of 43% when the image alignment is added to the model. However, it can be seen that the estimation errors are still higher than the results from the EigneNail model. Based on the results, The drop in the estimation error is much more prominent among the other three fingers than the Thumb, where the force estimation error is quite similar to the result from the initial model (with no alignment).

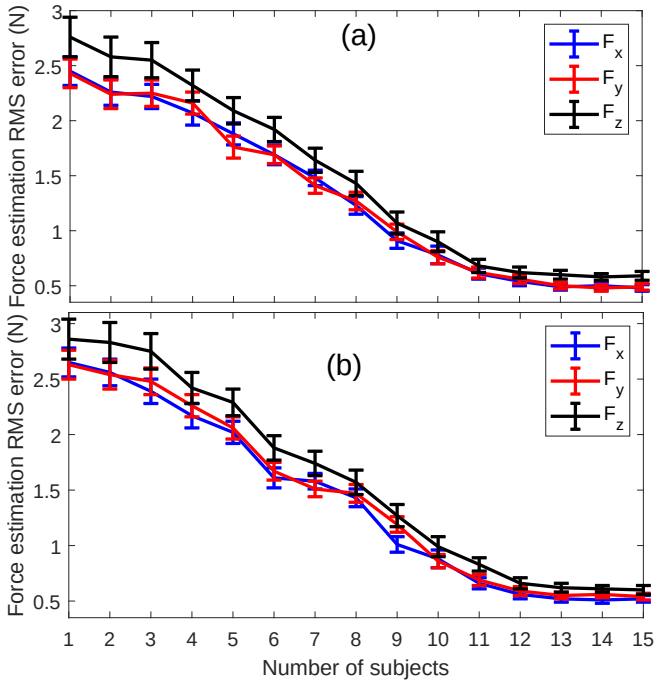

Fig. 5: Average force estimation error over five different random subject configuration with respect to the number of subjects in the training dataset. (a) Force estimation error change for the Fingers model. (b) Force estimation error change for the Thumb model.

Because of the different shape and size of the thumb compared to the other fingers (different sizes of the regions where the coloration patterns occur), it could be expected that the model's performance would degrade when tested on the thumb's images. The number of thumb images in the dataset is three times smaller than the other three similar fingers, resulting in poor performance in force estimation for the thumb. To resolve this problem, we decided to use two different force estimation models, including one for the thumb and one for the other three fingers. This solution also makes sense from the grasping perspective as humans tend to place their thumb on a different side of an object [25], which requires a second camera to look at the thumb. The results for the two models are shown in Table I, where the thumb model is trained with the thumb data only, and the finger model (the model for the index, middle, and ring fingers) is trained with the remaining data. According to Table I, the force estimation errors are comparable to results from the baseline EigenNail model.

To study the effect of subject change on the force estimation accuracy, we first randomly chose the data from 3 subjects for the test. Then, we trained the model with data from the remaining 15 subjects so that a new subject's data was added to the training dataset at each step. This procedure was repeated for both the thumb and the finger models. This process was repeated 5 times with different arrangements of subjects in the test and the training pools. The performance of the model when trained with different subjects is shown in Fig. 5. Based on the results in Fig. 5, it can be seen that after having enough subject variation in the training dataset, we can get the same level of accuracy reported in Table I. Additionally, we performed a Tukey post-

TABLE II: The average RMS force estimation results during a 10-second grasping experiment. Each column shows the average force estimation error in (N) along each direction, while each row shows the results for each individual fingers.

	F_x (N)	F_y (N)	F_z (N)
Index	0.46 ± 0.03	0.48 ± 0.02	0.62 ± 0.03
Middle	0.47 ± 0.03	0.50 ± 0.02	0.60 ± 0.02
Ring	0.47 ± 0.02	0.49 ± 0.02	0.57 ± 0.03
Thumb	0.49 ± 0.03	0.47 ± 0.03	0.58 ± 0.03

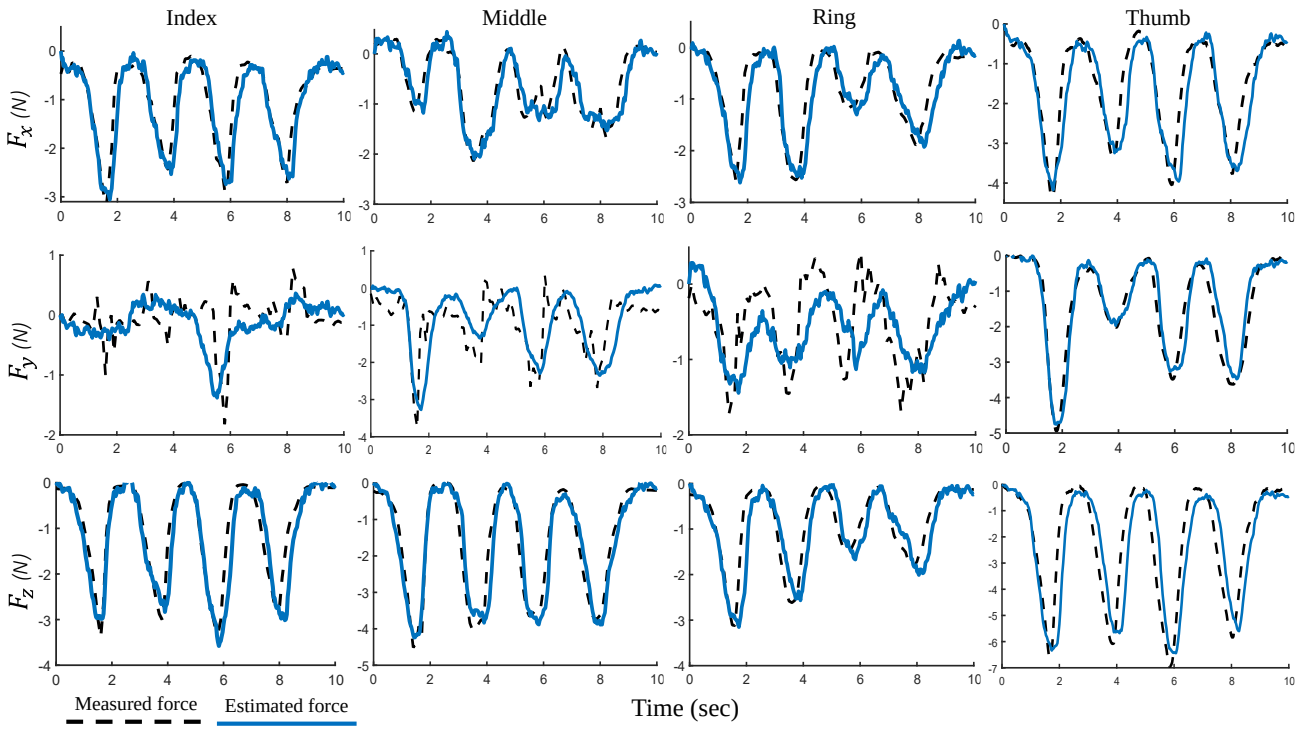

Fig. 6: Estimated 3D forces vs. measured forces during a grasping task. The human subject was instructed to grasp an instrumented object and apply some arbitrary force levels for 10 seconds similar to the task described in [16]. The forces were estimated in real-time at 30 FPS using a stationary camera facing towards one side of the objects with three fingers (index, middle, and ring) in the field of view.

hoc pairwise comparison test among the different number of subjects to show at which number the error becomes unchanged. The results indicate that there is a statistically significant error difference between $N \geq 11$ and $N < 11$ for the finger model ($p < 0.001$), and between $N \geq 12$ and $N < 12$ for the thumb model ($p < 0.001$).

Finally, the model was integrated with the finger detection and tracking module for real-time force estimation from camera frames. For this experiment, we used the same setup that was described in [16] with the only difference being that the object and the camera were stationary. Fig. 6 shows the measured vs. the estimated grasp forces over 10 seconds. The estimation was performed at 30 frames per second. Table II shows the average force estimation RMS error (over 10 seconds) for each individual finger along the x, y ,and z axes. From Table II, it can be seen that the force estimation error during a dynamic grasping experiment has increased by 6% along x axis, 8% along y axis, and 5% along z axis, respectively compared to the static grasping results.

V. CONCLUSIONS

This paper presented a novel approach for real-time 3D human tactile force sensing via fingernail imaging, which enables robotic systems to estimate the interaction forces using vision only. This method eliminates the need for costly and intrusive force sensors in HRI applications, enabling them to fuse force sensing with posture estimation for human intent prediction through an entirely vision-based system. In addition, the introduced vision-based force sensing technique enables the manipulators to learn to grasp synergies directly from human demonstrations in an end-to-end way.

We presented an image alignment approach based on STN to increase the accuracy of force estimations. Based on the experimental results, it can recover the geometrical transformations in the image with an accuracy of about less than 1% RMS pixel error. It has been shown that the image alignment can increase the force estimation accuracy by an average of 43% compared to the raw images. We also introduced two force estimation models (one for the thumb and one for the three other fingers), which estimate the 3D forces with the maximum RMS error of 7.1% (for the entire range of force levels) along all three directions among all four fingers. Finally, we integrated the force estimation model with a finger detection and tracking model, which runs at 30 FPS. This entire model is used for real-time tactile force estimation of each individual finger from a live camera feed.

Future works include implementing the force estimation model on an HRI platform where multiple robotic arms can follow the human hand and sense the grasping or manipulation forces applied by the fingertips, similar to the setup that was introduced in [16]. Furthermore, the grasp force estimating model will be incorporated with a 3D posture estimation model, which together can provide comprehensive information about the human state during an HRI task.

REFERENCES

[1] A. Billard and D. Kragic, "Trends and challenges in robot manipulation," *Science*, vol. 364, no. 6446, 2019.

[2] V. Villani, F. Pini, F. Leali, and C. Secchi, "Survey on human–robot collaboration in industrial settings: Safety, intuitive interfaces and applications," *Mechatronics*, vol. 55, pp. 248–266, 2018.

[3] A. S. Gailey, S. B. Godfrey, R. E. Breighner, K. L. Andrews, K. D. Zhao, A. Bicchi, and M. Santello, "Grasp performance of a soft synergy-based prosthetic hand: a pilot study," *IEEE Transactions on Neural Systems and Rehabilitation Engineering*, vol. 25, no. 12, pp. 2407–2417, 2017.

[4] H. Su, C. Yang, G. Ferrigno, and E. De Momi, "Improved human–robot collaborative control of redundant robot for teleoperated minimally invasive surgery," *IEEE Robotics and Automation Letters*, vol. 4, no. 2, pp. 1447–1453, 2019.

[5] S. Li and X. Zhang, "Implicit intention communication in human–robot interaction through visual behavior studies," *IEEE Transactions on Human-Machine Systems*, vol. 47, no. 4, pp. 437–448, 2017.

[6] K. Fujii, G. Gras, A. Salerno, and G.-Z. Yang, "Gaze gesture based human robot interaction for laparoscopic surgery," *Medical image analysis*, vol. 44, pp. 196–214, 2018.

[7] P. Schydlo, M. Rakovic, L. Jamone, and J. Santos-Victor, "Anticipation in human-robot cooperation: A recurrent neural network approach for multiple action sequences prediction," in *2018 IEEE International Conference on Robotics and Automation (ICRA)*, pp. 5909–5914, IEEE, 2018.

[8] R. M. Aronson, T. Santini, T. C. Kübler, E. Kasneci, S. Srinivasa, and H. Admoni, "Eye-hand behavior in human-robot shared manipulation," in *Proceedings of the 2018 ACM/IEEE International Conference on Human-Robot Interaction*, pp. 4–13, 2018.

[9] S. Li, L. Zhang, and X. Diao, "Deep-learning-based human intention prediction using rgb images and optical flow," *Journal of Intelligent & Robotic Systems*, vol. 97, no. 1, pp. 95–107, 2020.

[10] A. Zunino, J. Cavazza, R. Volpi, P. Morerio, A. Cavallo, C. Becchio, and V. Murino, "Predicting intentions from motion: The subject-adversarial adaptation approach," *International Journal of Computer Vision*, vol. 128, no. 1, pp. 220–239, 2020.

[11] S. Ma, L. Sigal, and S. Sclaroff, "Learning activity progression in lstms for activity detection and early detection," in *Proceedings of the IEEE conference on computer vision and pattern recognition*, pp. 1942–1950, 2016.

[12] C. Fermüller, F. Wang, Y. Yang, K. Zampogiannis, Y. Zhang, F. Barranco, and M. Pfeiffer, "Prediction of manipulation actions," *International Journal of Computer Vision*, vol. 126, no. 2, pp. 358–374, 2018.

[13] V. Adeli, E. Adeli, I. Reid, J. C. Niebles, and H. Rezatofighi, "Socially and contextually aware human motion and pose forecasting," *IEEE Robotics and Automation Letters*, vol. 5, no. 4, pp. 6033–6040, 2020.

[14] A. Naceri, A. Moscatelli, M. Santello, and M. O. Ernst, "Coordination of multi-digit positions and forces during unconstrained grasping in response to object perturbations," in *2014 IEEE Haptics Symposium (HAPTICS)*, pp. 35–40, IEEE, 2014.

[15] E. Battaglia, M. Bianchi, A. Altobelli, G. Grioli, M. G. Catalano, A. Serio, M. Santello, and A. Bicchi, "Thimblesense: a fingertip-wearable tactile sensor for grasp analysis," *IEEE transactions on haptics*, vol. 9, no. 1, pp. 121–133, 2015.

[16] N. Fallahinia and S. A. Mascaro, "Comparison of constrained and unconstrained human grasp forces using fingernail imaging and visual

[20] Y. Sun, J. M. Hollerbach, and S. A. Mascaro, "Imaging the finger force direction," in *2007 IEEE Conference on Computer Vision and Pattern Recognition*, pp. 1–6, IEEE, 2007.

servoing," in *2020 IEEE International Conference on Robotics and Automation (ICRA)*, pp. 2668–2674, IEEE, 2020.

[17] M. Santello and J. F. Soechting, "Force synergies for multifingered grasping," *Experimental brain research*, vol. 133, no. 4, pp. 457–467, 2000.

[18] Y. Sun, J. M. Hollerbach, and S. A. Mascaro, "Measuring fingertip forces by imaging the fingernail," in *2006 14th Symposium on Haptic Interfaces for Virtual Environment and Teleoperator Systems*, pp. 125–131, IEEE, 2006.

[19] Y. Sun, J. M. Hollerbach, and S. A. Mascaro, "Predicting fingertip forces by imaging coloration changes in the fingernail and surrounding skin," *IEEE Transactions on Biomedical Engineering*, vol. 55, no. 10, pp. 2363–2371, 2008.

[21] Y. Sun, J. M. Hollerbach, and S. A. Mascaro, "Estimation of fingertip force direction with computer vision," *IEEE Transactions on Robotics*, vol. 25, no. 6, pp. 1356–1369, 2009.

[22] T. Grieve, L. Lincoln, Y. Sun, J. M. Hollerbach, and S. A. Mascaro, "3d force prediction using fingernail imaging with automated calibration," in *2010 IEEE Haptics Symposium*, pp. 113–120, IEEE, 2010.

[23] T. R. Grieve, J. M. Hollerbach, and S. A. Mascaro, "Optimizing fingernail imaging calibration for 3d force magnitude prediction," *IEEE transactions on haptics*, vol. 9, no. 1, pp. 69–79, 2015.

[24] N. Fallahinia and S. A. Mascaro, "The effect of contact surface curvature on the accuracy of fingernail imaging for tactile force measurement," in *2020 IEEE Haptics Symposium (HAPTICS)*, pp. 760–766, IEEE, 2020.

[25] N. Fallahinia, S. Harris, and S. Mascaro, "Grasp force sensing using visual servoing and fingernail imaging," in *Dynamic Systems and Control Conference*, vol. 51890, p. V001T04A010, American Society of Mechanical Engineers, 2018.

[26] N. Chen, G. Westling, B. B. Edin, and P. van der Smagt, "Estimating fingertip forces, torques, and local curvatures from fingernail images," *Robotica*, vol. 38, no. 7, pp. 1242–1262, 2020.

[27] T.-H. Pham, N. Kyriazis, A. A. Argyros, and A. Kheddar, "Hand-object contact force estimation from markerless visual tracking," *IEEE transactions on pattern analysis and machine intelligence*, vol. 40, no. 12, pp. 2883–2896, 2017.

[28] M. Jaderberg, K. Simonyan, A. Zisserman, *et al.*, "Spatial transformer networks," *Advances in neural information processing systems*, vol. 28, pp. 2017–2025, 2015.

[29] T. R. Grieve, J. M. Hollerbach, and S. A. Mascaro, "3-d fingertip touch force prediction using fingernail imaging with automated calibration," *IEEE Transactions on Robotics*, vol. 31, no. 5, pp. 1116–1129, 2015.

[30] M. Sandler, A. Howard, M. Zhu, A. Zhmoginov, and L.-C. Chen, "Mobilenetv2: Inverted residuals and linear bottlenecks," in *Proceedings of the IEEE conference on computer vision and pattern recognition*, pp. 4510–4520, 2018.

[31] W. Liu, D. Anguelov, D. Erhan, C. Szegedy, S. Reed, C.-Y. Fu, and A. C. Berg, "Ssd: Single shot multibox detector," in *European conference on computer vision*, pp. 21–37, Springer, 2016.

[32] J. Bai, F. Lu, K. Zhang, *et al.*, "Onnx: Open neural network exchange." https://github.com/onnx/onnx, 2019.

[33] N. Fallahinia and S. A. Mascaro, "Feasibility study of force measurement for multi-digit unconstrained grasping via fingernail imaging and visual servoing," *ASME Letters in Dynamic Systems and Control*, vol. 1, no. 2, 2021.

[34] M. Afifi, "11k hands: gender recognition and biometric identification using a large dataset of hand images," *Multimedia Tools and Applications*, 2019.